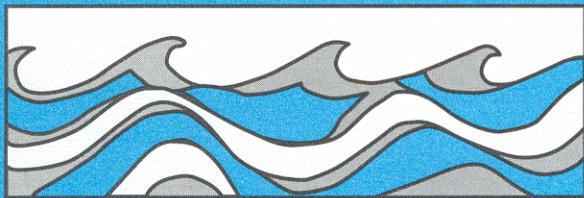


University of Washington
Department of Civil and Environmental Engineering



GROUNDWATER SEEPAGE PAST SHARP AND ROUNDED CORNERS

Bruce W. Hunt
Achi Mohamed Ishaq



Water Resources Series
Technical Report No. 30
June 1971

Seattle, Washington
98195

Department of Civil Engineering
University of Washington
Seattle, Washington 98195

GROUNDWATER SEEPAGE PAST SHARP AND ROUNDED
CORNERS

Bruce W. Hunt
Achi Mohamed Ishaq

Water Resources Series
Technical Report No. 30

June 1971

GROUNDWATER SEEPAGE PAST SHARP AND ROUNDED CORNERS

by Bruce W. Hunt and Achi Mohamed Ishag

KEY WORDS. - Groundwater^{*}, Seepage, Porous Media, Darcy Flow^{*}

ABSTRACT . - An experimental investigation was undertaken with two sand-box models to study the piezometric head distributions for groundwater seepage in the neighborhood of impervious boundaries with sharp and rounded corners. Piezometric head distributions were measured for flow which accelerated after passing a sharp corner, for flow which decelerated after passing a sharp corner, for flow which accelerated after passing a rounded corner, and for flow which decelerated after passing a rounded corner. These experimental piezometric head distributions were then compared with the theoretical piezometric head distributions calculated from Darcy's law. The results of this comparison indicate that there is better agreement between theory and experiment for flow past a rounded corner than for flow past a sharp corner and that the best agreement in either case is obtained for flow which decelerates after passing a sharp or rounded corner. In addition it was found that dimensionless piezometric head distributions were not identical for the decelerating and accelerating flows. Since Darcy's law predicts that the dimensionless piezometric head distributions should be identical, and since Reynolds numbers were less than unity for the flows past the rounded corner, it was concluded that either Darcy's law does not accurately describe seepage in regions of rapid acceleration or else experimental errors must account for the rather large disagreement between experiment and theory.

GROUNDWATER SEEPAGE PAST SHARP AND ROUNDED
CORNERS

A completion Report of Project Number
A-041-WASH
of the Office of Water Resources Research
Under Annual Allotment Agreement Number
14-31-0001-3248
July 1, 1970 to June 30, 1971

University of Washington
Seattle, Washington 98105

Bruce W. Hunt and Achi Mohamed Ishaq
July 1971

TABLE OF CONTENTS

<u>CHAPTER</u>		<u>PAGE</u>
I	INTRODUCTION	1
II	OBJECTIVES	4
III	THEORETICAL ANALYSIS	5
	1. Darcy's law and its range of validity	5
	2. Variation of Reynolds number along a boundary	6
	3. Laplace equation and solutions	7
	4. Electrical analogy	8
	5. The analog field plotter	8
IV	EXPERIMENTAL INVESTIGATION	10
	1. Construction of Models	10
	2. Procedure	15
V	RESULTS	17
VI	DISCUSSION AND CONCLUSIONS	32
	BIBLIOGRAPHY	34

LIST OF FIGURES

<u>FIGURE</u>		<u>PAGE</u>
1.	Circuit Diagram of Analog Field Plotter	9
2.	Schematic Diagram of Model with Sharp Corner	11
3.	Schematic Diagram of Model with Rounded Corner	11
4.	Photograph of Model with Sharp Corner	12
5.	Photograph of Model with Rounded Corner	13
6.	Plexiglass Case with Sharp Corner	14
7.	Plexiglass Case with Rounded Corner	14
8.	Rounded-Corner Model - Distribution of Manometer Taps	18
9.	Sharp-Corner Model - Distribution of Manometer Taps	21
10.	Diverging Flow Past a Rounded Corner - Distri- bution of Theoretical and Experimental Equipotential Lines	25
11.	Converging Flow Past a Rounded Corner - Distri- bution of Theoretical and Experimental Equipotential Lines	26
12.	Diverging Flow Past a Sharp Corner - Distri- bution of Theoretical and Experimental Equipotential Lines	27
13.	Converging Flow Past a Sharp Corner - Distri- bution of Theoretical and Experimental Equipotential Lines	28

<u>FIGURE</u>		<u>PAGE</u>
14.	Diverging Flow Past Rounded and Sharp Corners - Distribution of Experimental Equi- potential Lines	29
15.	Converging Flow Past Rounded and Sharp Corners - Distribution of Experimental Equi- potential Lines	30
16.	Variation of Reynolds Number along the Boundary for Diverging and Converging Flow Past a Rounded Corner	31

LIST OF TABLES

<u>TABLE</u>		<u>PAGE</u>
I	Converging Flow Past a Rounded Corner - Manometer Readings	19
II	Diverging Flow Past a Rounded Corner - Manometer Readings	20
III	Converging Flow Past a Sharp Corner - Manometer Readings	22
IV	Diverging Flow Past a Sharp Corner - Manometer Readings	23
V	Reynolds Numbers and Velocities	24

NOTATION

The following symbols are used in this thesis:

a	=	a constant;
b	=	a constant;
c	=	a constant;
D	=	average diameter of glass beads;
g	=	gravitational acceleration;
h	=	piezometric head = $(\frac{p}{\gamma} + z)$;
i	=	hydraulic gradient;
I	=	current;
k	=	coefficient of permeability;
P	=	pressure;
Re	=	Reynolds number;
u	=	velocity in the x direction;
v	=	velocity in the y direction;
w	=	velocity in the z direction;
V	=	discharge velocity;
x	=	distance measured in the x direction;
y	=	distance measured in the y direction;
z	=	distance measured in the vertical direction;
ρ	=	density of fluid;
μ	=	coefficient of dynamic viscosity;
γ	=	specific weight;
σ	=	conductivity.
ϕ	=	potential function (velocity potential)

ACKNOWLEDGMENTS

The work upon which this report is based was supported by funds provided by the United States Department of the Interior, Office of Water Resources Research Act of 1964.

CHAPTER I

INTRODUCTION

In 1856 the well-known French engineer Darcy [3]^{*} was interested in the flow characteristics of sand filters. Darcy had to resort to an experimental study of the problem, and thereby laid the real foundation for the qualitative theory of the flow of homogeneous fluids through a porous media. His classical experiments gave very simple results -- that the rate of flow, Q , of water through the filter bed is directly proportional to the area, A , of the sand the the piezometric head difference, Δh , between the fluid heads at the inlet and outlet faces of the bed and is inversely proportional to the thickness, L , of the bed. This may be expressed analytically as

$$Q = \frac{cA\Delta h}{L} \dots\dots\dots (1)$$

where c is a constant characteristic of the sand.

In 1863 Dupuit [4] carried out the first theoretical investigation of seepage based on Darcy's law. He made two important assumptions in his theory: (1) that for small inclinations of the line of seepage the streamlines can be taken as horizontal (2) that the hydraulic gradient was equal to the slope of the free surface and was invariant with depth.

In 1889, the first general theory and differential equations of seepage were formulated by the eminent Russian mathematician and mechanist N. E. Zhukovskii [22]. His theory showed that, for any flow which satisfied Darcy's law, the piezometric head satisfied the Laplace equation.

^{*}Figures in brackets refer to references at the end of the thesis.

$$\frac{\partial^2 h}{\partial x^2} + \frac{\partial^2 h}{\partial y^2} + \frac{\partial^2 h}{\partial z^2} = 0 \dots\dots\dots(2)$$

Zhukovskii also pointed out the mathematical analogy between seepage and heat transfer.

Since the formulation of the general theory of seepage by Zhukovskii, countless numbers of experiments have been carried out in many nations to verify the results of Darcy and Zhukovskii for relatively low Reynolds numbers.

Laplace's equation is the simplest and most studied elliptic partial differential equation in mathematical physics. This has resulted in a vast number of mathematical solutions to particular seepage problems. However, a large majority of these solutions have at least one common weakness: that is, sharp corners in the geometry of flow boundaries which lead to infinite flow velocities in the mathematical model. As pointed out by Harr [6], since flow velocities (and thus Reynolds numbers) in the physical model also become large (although finite) at these points, this simply means that Darcy's law is no longer valid in the region of these mathematical singularities. This deviation from Darcy's law near the sharp corner modifies the entire flow field and, as pointed out, by Hunt [8] can lead to a considerable discrepancy between calculated and experimental results. One of the objectives of this research is to investigate in detail this experimental deviation of Darcy's law in the vicinity of a sharp corner, and then to investigate the effect of streamlining the corner by rounding it.

Many investigators in this century have concerned themselves with the experimental and analytical study of nonlinear seepage for relatively high Reynolds numbers [1], [18], [12]. Most of the experimental studies have been made upon one-dimensional flows between parallel boundaries, although one relatively recent experimental study [20] was concerned with the nonlinear seepage between converging streamlines. The analogous flow between diverging streamlines has yet to be studied.

Analytical studies have largely been concerned with developing numerical techniques for solving various partial differential equations which have been proposed as mathematical models for nonlinear seepage. However, the complexity of these nonlinear equations makes exact solutions impossible to obtain and numerical solutions both costly and difficult. Furthermore, not enough is yet known about these mathematical models to assess the strengths, weakness, and best uses of each. Since any equation for nonlinear flow which will be used in the future for engineering computation should be capable of modeling flow around a sharp corner with reasonable accuracy, the experimental results of this study should be useful to other investigators for testing the validity of various mathematical models of nonlinear seepage.

CHAPTER II

OBJECTIVES

The following are the primary objectives of this study:

1. To obtain a qualitative understanding of the way in which experimental pressures deviate from those calculated from Darcy's law in the neighborhood of sharp and rounded corners.

2. To provide detailed experimental results which could be used by other investigators to test the validity of various mathematical models of nonlinear seepage.

CHAPTER III

THEORETICAL ANALYSIS

1. Darcy's law and its range of validity. - The relationship between the hydraulic gradient and the discharge velocity is given by Darcy's law

$$V = ki \dots \dots \dots (3)$$

$$= -k \frac{dh}{ds}$$

where V = discharge velocity

k = coefficient of permeability

i = the negative hydraulic gradient

$$= - \frac{dh}{ds}$$

As stated by Harr [6], Darcy's law is a statistical, macroscopic equivalent of the Navier-Stokes equations of motion for viscous groundwater flow.

Though Darcy's law in no way describes the situation within an individual pore, it has been shown experimentally in many cases to give accurate macroscopic results for the so-called "creeping flows". The criterion of its validity is furnished by the Reynolds number

$$Rr = \frac{VD\rho}{\mu} \dots \dots \dots (4)$$

where

V = discharge velocity

D = average diameter of granular material

ρ = density of fluid

μ = coefficient of dynamic viscosity

Slichter [16] determined that Darcy's law does not hold for high Reynolds numbers. This resulted in Forchheimer [5] representing the hydraulic gradient by a nonlinear equation

$$i = av + bv^2 \dots \dots \dots (5)$$

where a and b are constants determined by the properties of the fluid and the medium. Later, Forchheimer added the factor cv^3 in order to obtain agreement with experimental results. A number of investigators | Lindquist [13], Ward [19], Maroon [11] | have verified Eq. 5 experimentally over a range of Reynolds numbers between 0 to 30.

Missbach [10] suggested the form

$$i = cv^m \dots \dots \dots (6)$$

where c = a constant determined by the properties of the fluid and medium

and m = an exponent lying between 1 and 2.

Equation 6 is empirical and has been used by specifying different values of c and m to fit experimental results [18].

Almost all the investigators agree that Darcy's law in its original form is valid for Reynolds numbers less than unity

$$\frac{vD_p}{\mu} \leq 1 \dots \dots \dots (7)$$

and that the transition from laminar to turbulent flow occurs in the range of Reynolds numbers between 1 and 12 [6].

2. Variation of Reynolds number along a boundary. - Assuming that Darcy's law is valid, velocities can be approximated along a boundary with the finite-difference equation

$$v = -k \frac{\Delta h}{\Delta s} \dots \dots \dots (8)$$

in which

V = discharge velocity along the boundary

k = coefficient of permeability

Δh = piezometric head drop along the boundary

Δs = increment of arc length along the boundary

Thus, the ratio of Reynolds numbers at any two points along the boundary is given by

$$\frac{R_1}{R_2} = \frac{v_1}{v_2} = \frac{\Delta h_1}{\Delta h_2} \frac{\Delta s_2}{\Delta s_1} \dots \dots \dots (9)$$

Equation 9 permits the approximate calculation of Reynolds number along a boundary if the Reynolds number at one point along the boundary is known.

3. Laplace's equation and solutions. - From the equation of continuity

$$\frac{\partial u}{\partial x} + \frac{\partial v}{\partial y} + \frac{\partial w}{\partial z} = 0 \dots \dots \dots (10)$$

and Darcy's law

$$u = \frac{\partial \phi}{\partial x} \dots \dots \dots (11)$$

$$v = \frac{\partial \phi}{\partial y} \dots \dots \dots (12)$$

$$w = \frac{\partial \phi}{\partial z} \dots \dots \dots (13)$$

is obtained the Laplace equation

$$\frac{\partial^2 \phi}{\partial x^2} + \frac{\partial^2 \phi}{\partial y^2} + \frac{\partial^2 \phi}{\partial z^2} = 0 \dots \dots \dots (14)$$

where

$$\phi = -k \left(\frac{P}{\gamma} + z \right) \dots \dots \dots (15)$$

The problem under consideration is two-dimensional so that $\phi = \phi(x, y)$ and the Laplace equation becomes

$$\nabla^2 \phi = \frac{\partial^2 \phi}{\partial x^2} + \frac{\partial^2 \phi}{\partial y^2} = 0 \dots\dots\dots (16)$$

Analytical solutions of this equation for different boundary conditions have been treated extensively in technical literature. Electrical analog solutions to steady-state seepage problems have also been shown to give exceptionally accurate results by many investigators [2],[7],[24],[21].

4. Electrical analogy. - The correspondence between the steady-state flow of water through a porous media and the steady-state flow of electricity in a conductor [6] is given below.

<u>Steady State Seepage</u>	<u>Electric Current</u>
Total head, h	Voltage, V
Coefficient of permeability, k	Conductivity, σ
Discharge velocity, v	Current, I
Darcy's law, $v = -k \text{ grad } h$	Ohm's law, $I = -\sigma \text{ grad } V$
Governing equation, $\nabla^2 h = 0$	Governing equation, $\nabla^2 V = 0$
Equipotential lines, $h = \text{const.}$	Equipotential lines, $V = \text{const.}$
Impervious boundary, $\frac{\partial h}{\partial n} = 0$	Insulated boundary, $\frac{\partial V}{\partial n} = 0$

From the above correspondence it is easily seen that the analogy between seepage and current flow is very close. Hence, to determine lines of equipotential in the problem under consideration, the flow domain may be replaced with an electrical conductor of similar geometry.

5. The analog field plotter. - A circuit diagram of an analog field plotter which is similar to that used in this study to determine the theoretical equipotential lines is shown in Fig. 1.

Conducting paper (Teledeltos) was cut precisely to half the scale of the model. Two strips of current-conducting, aluminum paint served as electrodes and, thus, modeled reservoirs of constant piezometric head in the experimental model. After setting the rectifier bridge at the required potential, the probe and null detector were used to trace the equipotential lines.

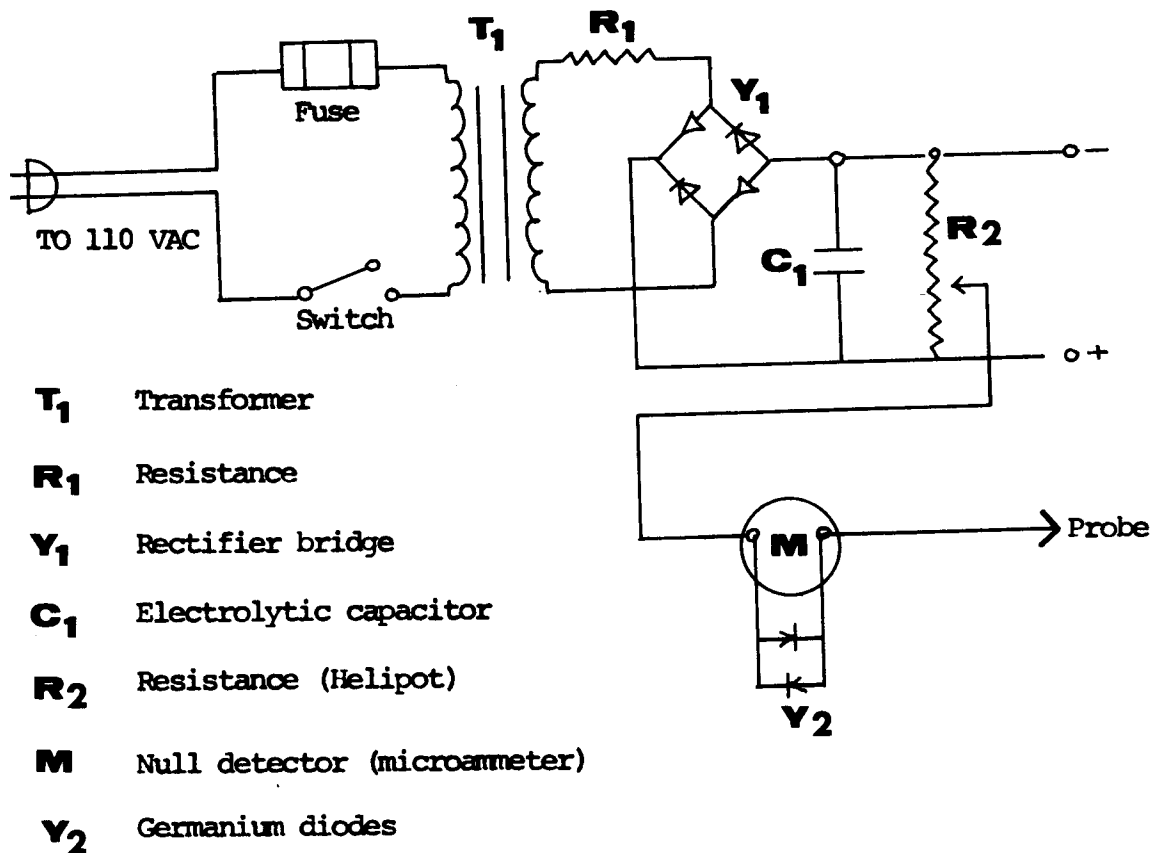


FIG. 1. - CIRCUIT DIAGRAM OF ANALOG FIELD PLOTTER

CHAPTER IV

EXPERIMENTAL INVESTIGATION

Schematic representations of the two models used for the investigation are shown in Figs. 2 and 3. Photographs of the same two models are shown in Figs. 4 and 5. These models were constructed and the experimental investigation was carried out at the Charles W. Harris Laboratory at the University of Washington.

1. Construction of Models. - The cases of these models were made of $\frac{1}{2}$ " thick Plexiglas as shown in Figs. 6 and 7. The sides and top were permanently bonded by means of metal screws and cement. A total of 79 and 61 manometer taps were installed in the tops of the models with the rounded and sharp corners, respectively. An additional 20 taps were added along the sides of the model with the sharp corner. These taps were all installed prior to assembling the cases.

Approximately 1.5 cu. ft. of fine glass beads with an average diameter of 0.0390 cm. were poured into a separate large pan and mixed thoroughly with Epoxy cement. The composition of the Epoxy cement consisted of 100 parts by weight of Epibond 1210 to 22 parts by weight of hardener 9615 (Furane). Wooden dummies coated with wax were placed in the positions of the end tanks. The mixture of glass beads and cement was then packed into the cases while taking extreme care to remove all air pockets in the aquifer. The cases were clamped firmly to a flat surface during the filling operation, and the models were allowed to cure for about 72 hours.

The wooden dummies were removed and a sheet of foam rubber soaked in rubber cement was placed on top of the consolidated aquifer. The Plexiglas bottom was then screwed onto the models after cement was placed on all the

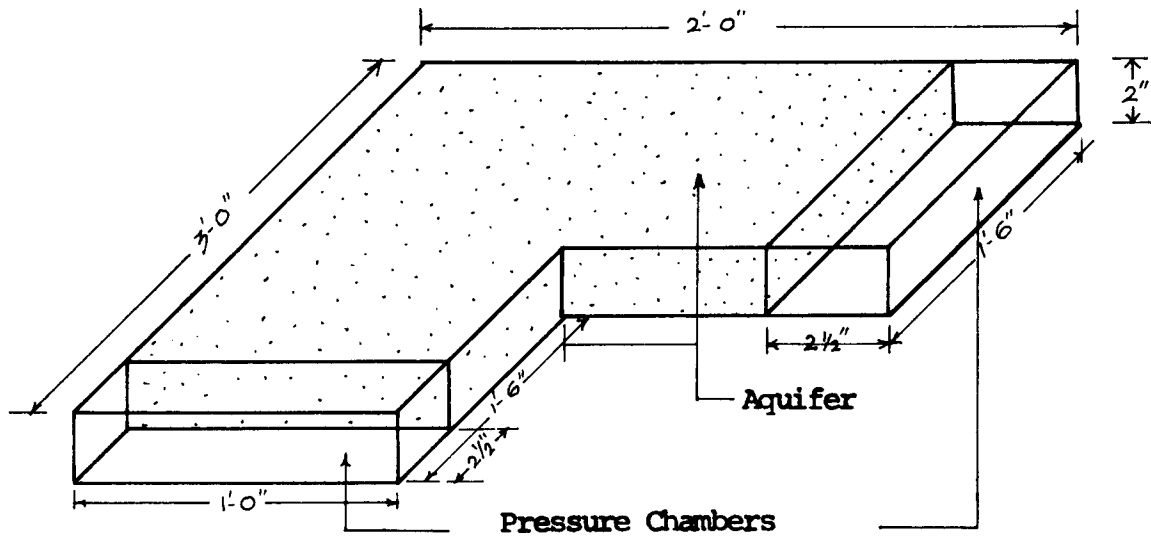


FIG. 2. - EXPERIMENTAL MODEL WITH SHARP CORNER

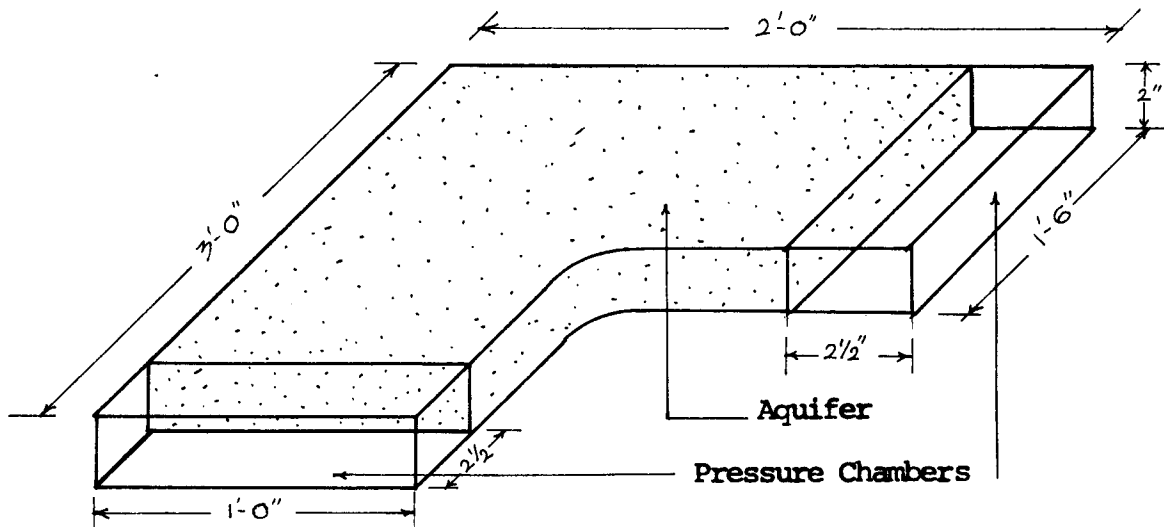


FIG. 3. - EXPERIMENTAL MODEL WITH ROUNDED CORNER

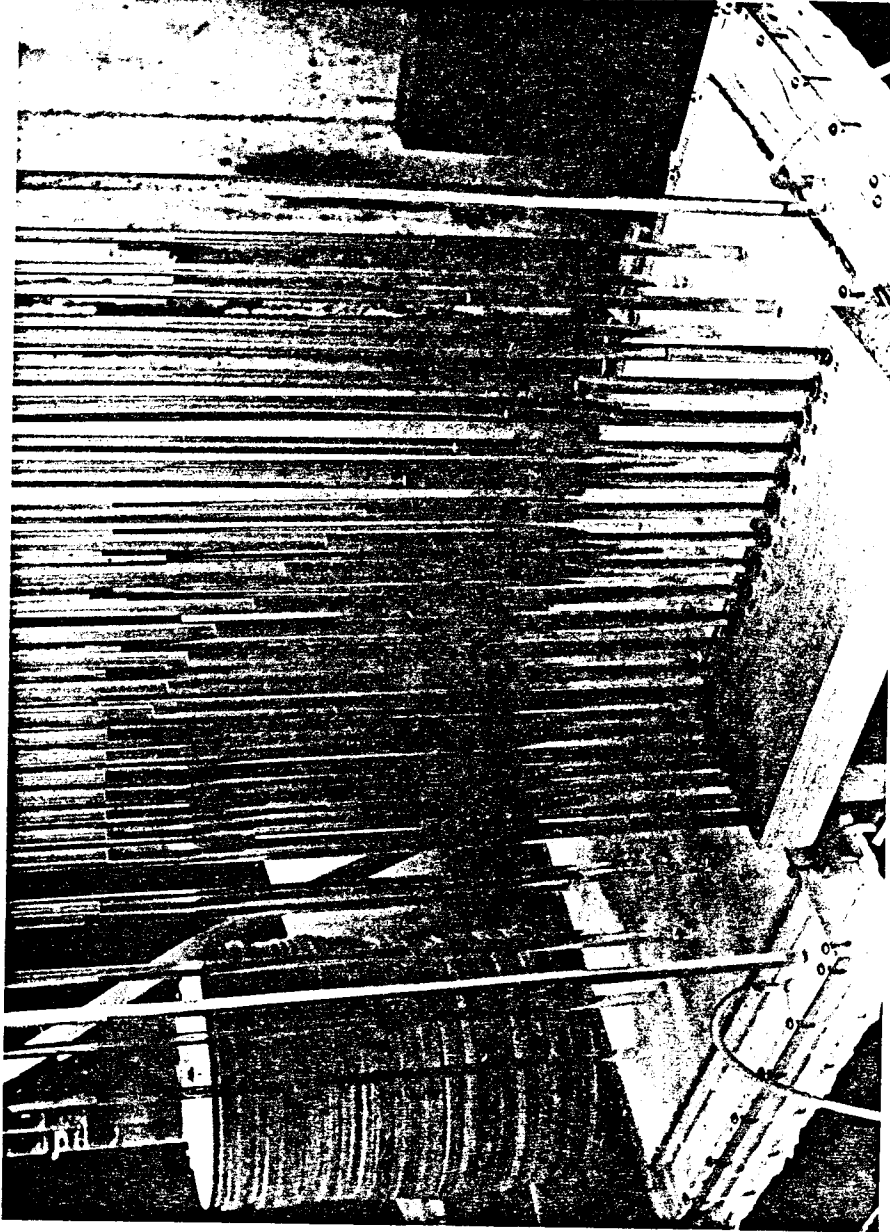


FIG. 4. - PHOTOGRAPH OF MODEL WITH SHARP CORNER

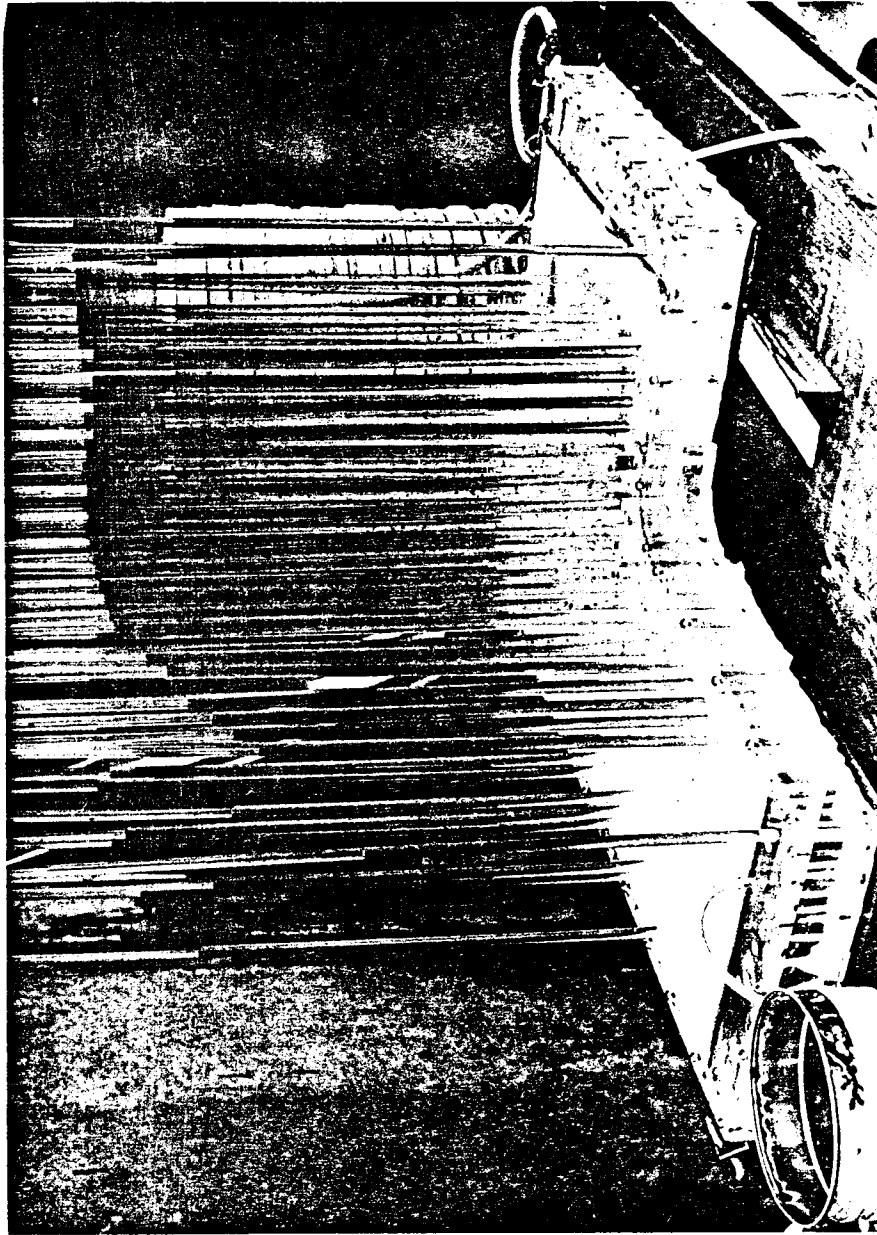


FIG. 5. - PHOTOGRAPH OF MODEL WITH ROUNDED CORNER

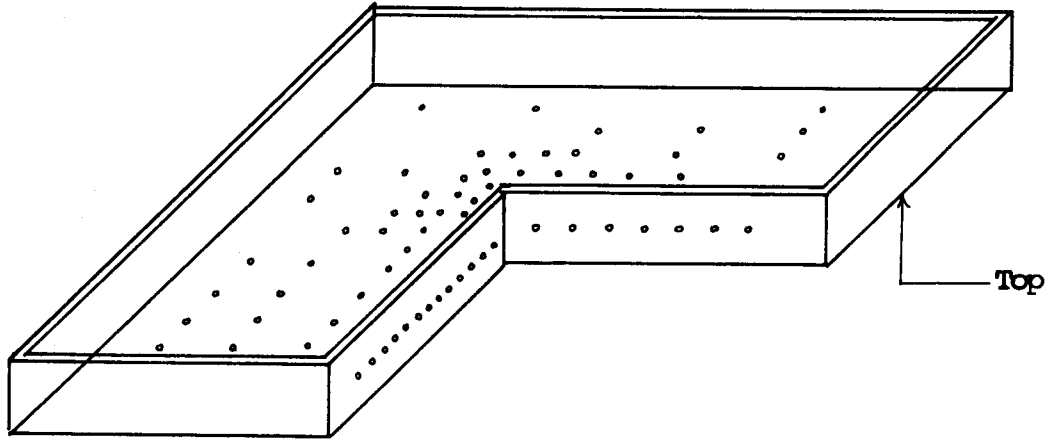


FIG. 6. - PLEXIGLAS CASE WITH SHARP CORNER IN INVERTED POSITION

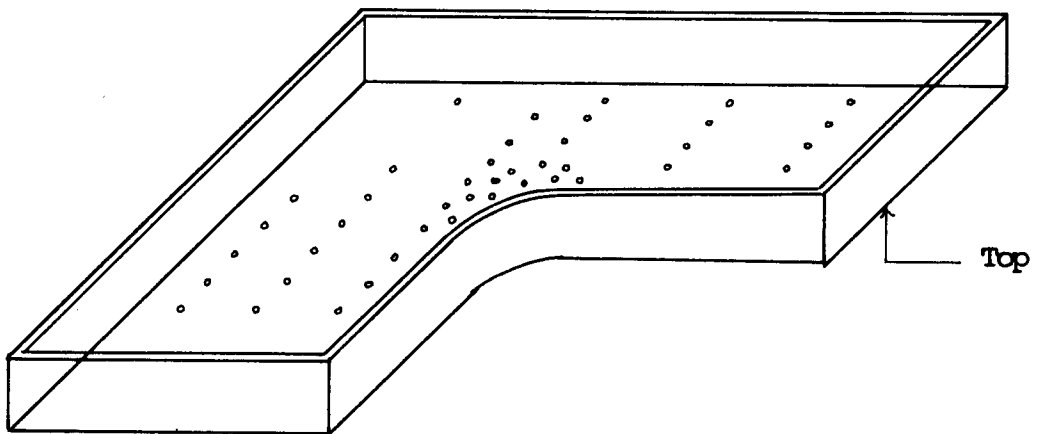


FIG. 7. - PLEXIGLAS CASE WITH ROUNDED CORNER IN INVERTED POSITION

seams to make the entire model watertight.

Finally, both models were turned upside down and placed on a flat surface for about 24 hours. Tenite tubing of inside diameter $7/16$ " was cut into 24" pieces and was cemented onto the manometer taps with Plexiglas cement. Inlet and outlet valves were fitted to the reservoirs.

A constant-head tank, 7" in diameter and 18" high, was constructed and placed on a wooden frame approximately 20" in height. Inflow for the overhead tank was taken from the city water supply lines, and the outlet from the overhead tank was connected to one of the tow end reservoirs of the model.

2. Procedure. - The model was initially levelled and then operated by opening the inlet valve very slightly while the outlet valve was kept closed. This was done in order to saturate the media very gradually and, thus, remove any air trapped in the porous media. When the media was saturated completely, the inlet valve was opened further to bring the water level at the inlet and outlet tanks to a higher common level. The levels in all the manometers were then checked to see if they were at the same level. This check was made to verify that the aquifer was completely saturated. The outlet valve was opened to bring down the level in the outlet reservoir to the desired height. A time period of about 15 to 20 minutes was allowed for the levels in the manometers to reach a steady state. The levels were then recorded with the aid of adjustable inside calipers and a 24-inch ruler taking the top of the model as the datum. The flow rate was determined by measuring the time required to collect a known volume of water at the outflow exit. Once a set of satisfactory readings was obtained for a particular direction of flow, the inlet valve was closed and the model was

drained completely. In order to reserve the direction of flow, the supply from the overhead tank was disconnected at the original inlet valve and reconnected to the outlet valve. The same procedure was adopted for the new direction of flow.

CHAPTER V

RESULTS

The distribution of manometer taps for the model with the rounded corner is shown in Fig. 8. Tables 1 and 2 show the manometer readings for the two directions of flow for this model. The distribution of manometer taps for the model with the sharp corner is shown in Fig. 9, and Tables 3 and 4 give the manometer readings for the two directions of flow. Table 5 shows the Reynolds numbers at the narrowest end reservoirs in the two models for the different experimental runs.

Equipotential lines were found by interpolating linearly between the measured values of piezometric head. The distributions of experimental equipotential lines thus obtained were compared with the theoretical equipotential lines obtained from the electrical analogy. These comparisons are shown in Figs. 10 and 11 for the flow past a rounded corner and in Figs. 12 and 13 for the flow past a sharp corner. The comparison of the distribution of equipotential lines for flow past a sharp and rounded corner is shown in Figs. 14 and 15. The variation of the experimental and theoretical Reynolds numbers along the sides of the model with a rounded corner is shown in Fig. 16.

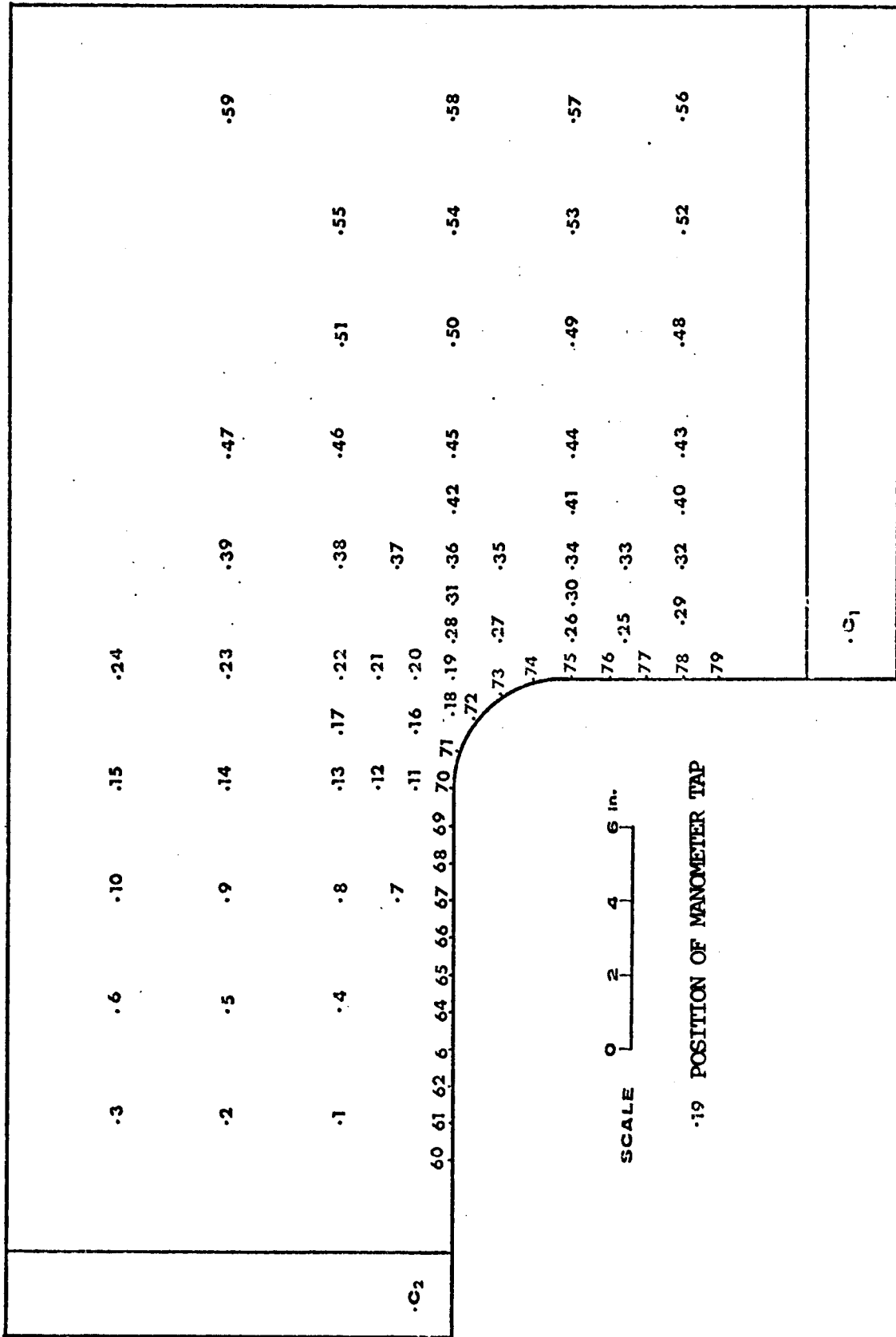


FIG. 8. - DISTRIBUTION OF MANOMETER TAPS FOR THE ROUNDED CORNER MODEL

TABLE I

FLOW PAST A ROUNDED CORNER

Flow from c_1 to c_2

Flow Rate = 9.5 cc/sec.

(= 0.58 cu.in./sec.)

Manometer No.	Head in.	Manometer No.	Head in.	Manometer No.	Head in.	Manometer No.	Head in.
c_1	14.50	21	11.84	42	12.20	63	8.68
1	6.96	22	11.82	43	12.82	64	9.32
2	6.96	23	11.84	44	12.32	65	9.72
3	7.00	24	11.68	45	12.30	66	9.96
4	9.40	25	12.56	46	12.12	67	10.44
5	9.28	26	12.30	47	12.16	68	10.70
6	9.00	27	12.10	48	12.82	69	10.94
7	10.40	28	12.04	49	12.32	70	11.06
8	10.40	29	12.82	50	12.20	71	11.70
9	10.36	30	12.30	51	12.26	72	11.80
10	10.14	31	12.08	52	12.82	73	11.98
11	11.28	32	12.82	53	12.32	74	12.10
12	11.24	33	12.58	54	12.20	75	12.32
13	11.24	34	12.30	55	12.28	76	12.44
14	11.20	35	12.15	56	12.82	77	12.66
15	11.05	36	12.10	57	12.32	78	12.80
16	11.70	37	12.06	58	12.20	79	13.00
17	11.66	38	12.00	59	12.20	c_2	2.40
18	12.74	39	11.98	60	5.88		
19	11.92	40	12.82	61	6.90		
20	11.90	41	12.32	62	8.06		

TABLE II

FLOW PAST A ROUNDED CORNER

Flow from c_2 to c_1 Flow Rate = 14.75 cc/sec.
(= 0.90 cu.in./sec.)

Manometer No.	Head in.	Manometer No.	Head in.	Manometer No.	Head in.	Manometer No.	Head in.
c_1	4.00	21	10.44	42	8.54	63	16.25
1	18.60	22	10.52	43	5.76	64	15.42
2	18.54	23	11.12	44	7.02	65	14.72
3	18.54	24	11.38	45	8.50	66	13.98
4	15.40	25	7.08	46	8.88	67	13.60
5	15.38	26	8.00	47	9.10	68	12.80
6	15.24	27	8.82	48	5.76	69	12.65
7	13.66	28	9.40	49	6.90	70	11.74
8	13.66	29	6.08	50	7.92	71	11.10
9	13.68	30	7.80	51	8.40	72	10.24
10	13.82	31	9.04	52	5.68	73	9.52
11	12.12	32	5.96	53	6.82	74	8.66
12	12.14	33	6.90	54	7.70	75	8.10
13	12.25	34	7.70	55	8.14	76	7.46
14	12.40	35	8.46	56	5.60	77	6.80
15	12.50	36	8.82	57	6.74	78	6.16
16	11.04	37	9.30	58	7.54	79	5.58
17	11.44	38	9.52	59	8.24	c_2	23.14
18	10.66	39	10.04	60	19.48		
19	9.84	40	5.80	61	18.56		
20	10.20	41	7.34	62	17.54		

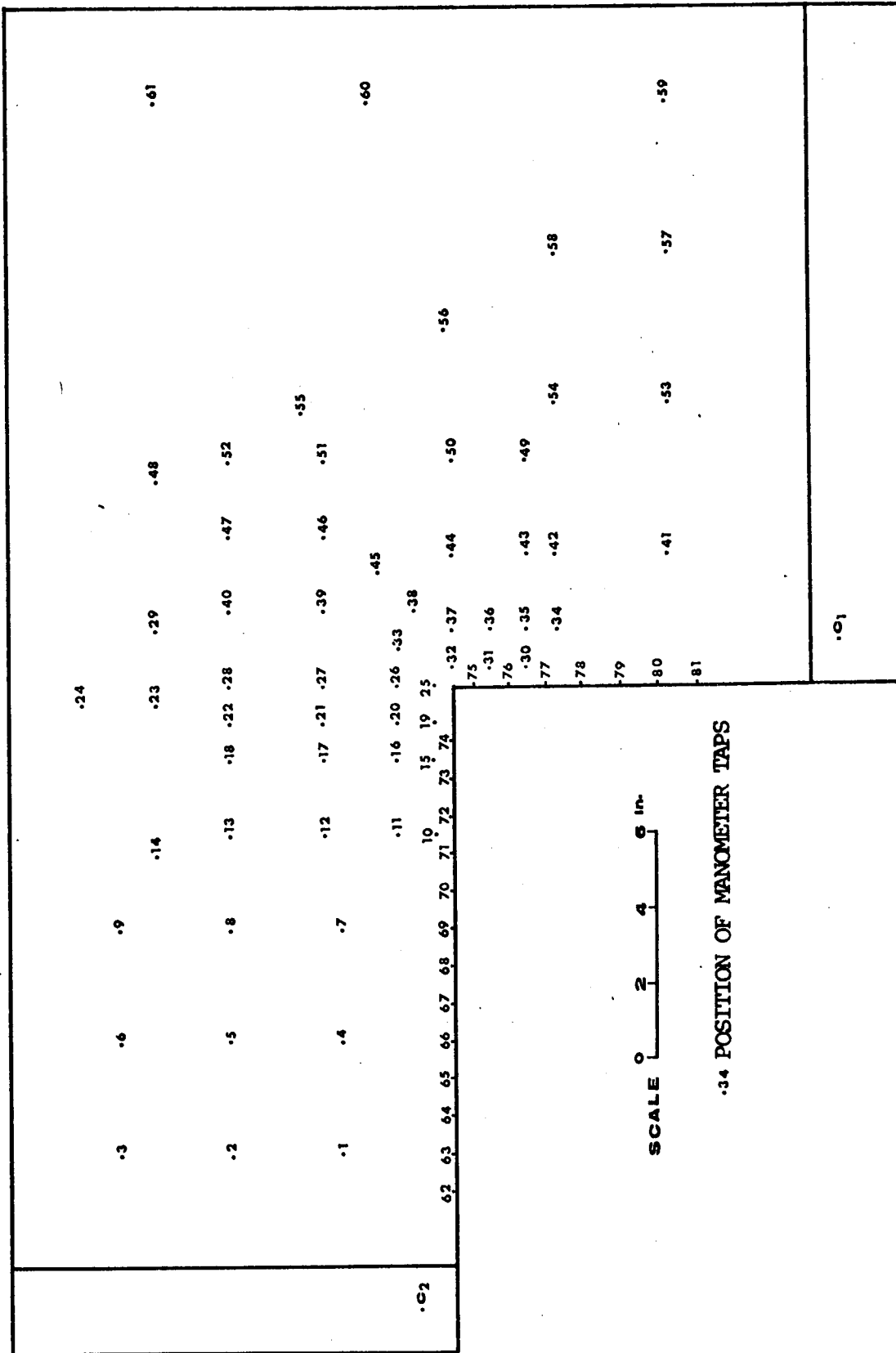


FIG. 9. DISTRIBUTION OF MANOMETER TAPS FOR THE SHARP CORNER MODEL

TABLE III

FLOW PAST A SHARP CORNER

Flow from c_1 to c_2

Flow Rate = 6.95 cc/sec.

(= 0.42 cu.in./sec.)

Manometer No.	Head in.	Manometer No.	Head in.	Manometer No.	Head in.	Manometer No.	Head in.
c_1	16.60	21	15.00	42	16.04	63	7.70
1	7.70	22	14.98	43	10.02	64	8.38
2	7.66	23	14.96	44	15.96	65	8.95
3	7.58	24	14.26	45	15.90	66	9.57
4	9.55	25	15.32	46	15.90	67	10.53
5	9.50	26	15.42	47	15.82	68	10.84
6	9.45	27	15.42	48	15.85	69	11.36
7	11.44	28	15.23	49	16.04	70	12.33
8	11.40	29	15.36	50	16.00	71	12.81
9	11.36	30	15.96	51	15.96	72	13.20
10	12.90	31	15.80	52	15.92	73	14.30
11	12.90	32	15.66	53	16.16	74	14.63
12	12.90	33	15.78	54	16.08	75	16.23
13	12.88	34	16.05	55	16.00	76	16.26
14	12.34	35	16.02	56	16.08	77	16.27
15	14.10	36	15.94	57	16.16	78	16.28
16	14.10	37	15.90	58	16.12	79	16.34
17	14.20	38	15.90	59	16.18	80	16.36
18	14.22	39	15.80	60	16.08	81	16.40
19	14.75	40	15.76	61	16.08	c_2	5.28
20	14.85	41	16.16	62	7.18		

TABLE IV

FLOW PAST A SHARP CORNER

Flow from c_2 to c_1 Flow Rate = 6.45 cc/sec.
(= 0.39 cu.in./sec.)

Manometer No.	Head in.	Manometer No.	Head in.	Manometer No.	Head in.	Manometer No.	Head in.
c_1	3.14	21	7.28	42	5.15	63	13.64
1	13.38	22	7.60	43	5.25	64	12.84
2	13.35	23	7.64	44	5.68	65	12.23
3	13.36	24	7.74	45	6.25	66	11.57
4	11.34	25	6.56	46	6.14	67	10.97
5	11.34	26	6.52	47	6.18	68	10.44
6	11.34	27	7.30	48	6.12	69	9.88
7	9.76	28	7.40	49	4.88	70	9.34
8	9.80	29	7.06	50	5.68	71	8.74
9	9.80	30	5.18	51	5.52	72	8.26
10	8.38	31	5.40	52	5.72	73	7.72
11	8.48	32	5.88	53	4.46	74	7.50
12	8.54	33	6.18	54	4.72	75	5.52
13	8.72	34	4.94	55	5.48	76	5.15
14	8.94	35	5.10	56	4.64	77	5.00
15	7.36	36	5.38	57	4.26	78	4.71
16	7.56	37	5.64	58	4.60	79	4.46
17	7.80	38	5.90	59	4.15	80	4.26
18	8.00	39	6.30	60	5.02	81	4.08
19	6.96	40	7.10	61	5.36	c_2	17.24
20	7.12	41	4.28	62	14.70		

TABLE V

REYNOLDS NUMBERS AND VELOCITIES

MODEL	FLOW	FLOW RATE in cm^3/sec .	REYNOLDS * NUMBER	VELOCITY in cm/sec .
ROUNDED CORNER	CONVERGING ($c_1 - c_2$)	9.5	0.204	0.061
	DIVERGING ($c_2 - c_1$)	14.75	0.317	0.095
SHARP CORNER	CONVERGING ($c_1 - c_2$)	6.95	0.150	0.045
	DIVERGING ($c_2 - c_1$)	6.45	0.139	0.042

* at a temperature of 58.5°F and at the narrow end of the model.

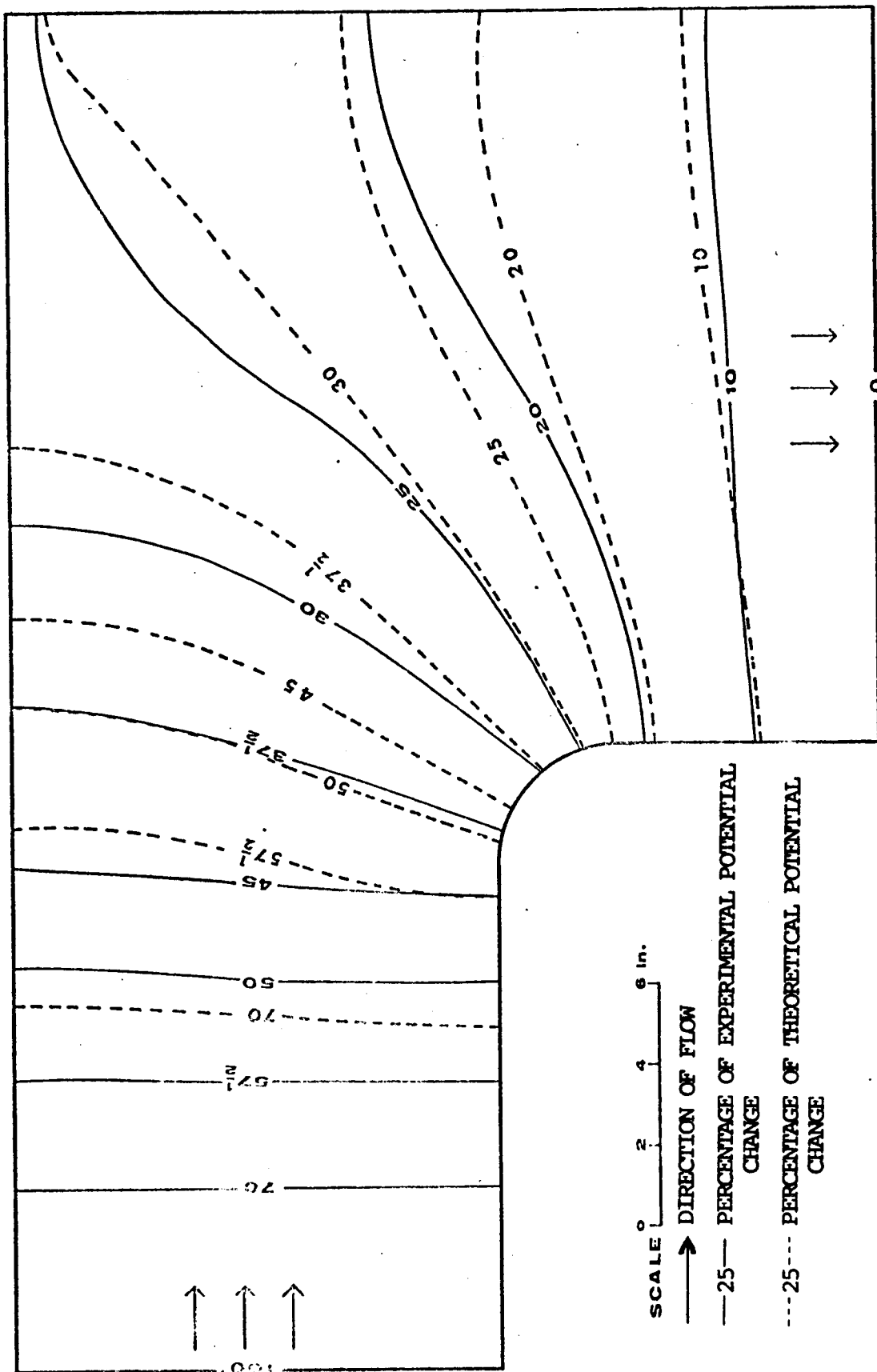


FIG. 10.-- DISTRIBUTION OF THEORETICAL AND EXPERIMENTAL EQUIPOTENTIAL LINES FOR FLOW PAST A ROUNDED CORNER

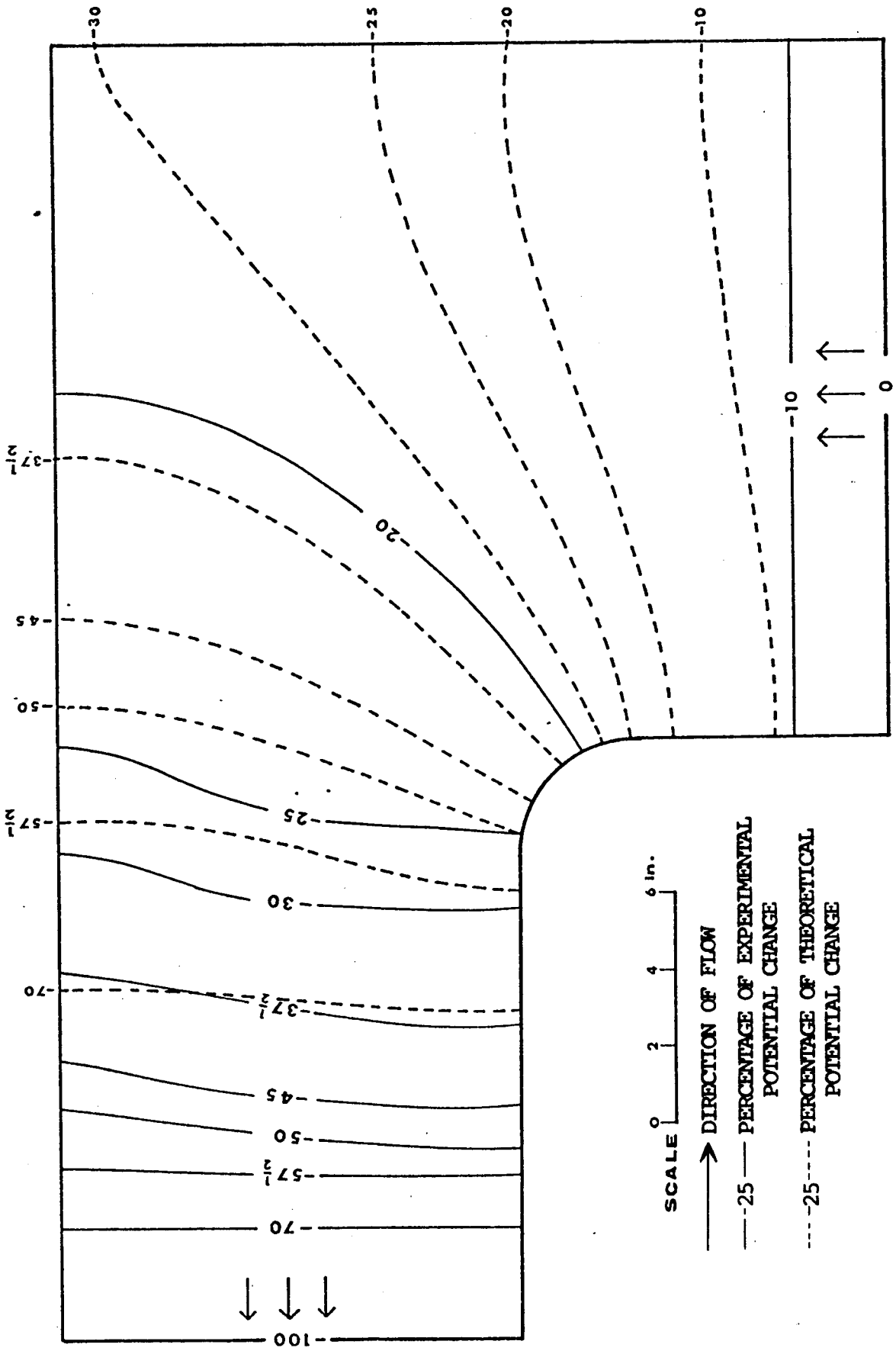


FIG. 11. DISTRIBUTION OF THEORETICAL AND EXPERIMENTAL EQUIPOTENTIAL LINES FOR FLOW PAST A ROUNDED CORNER

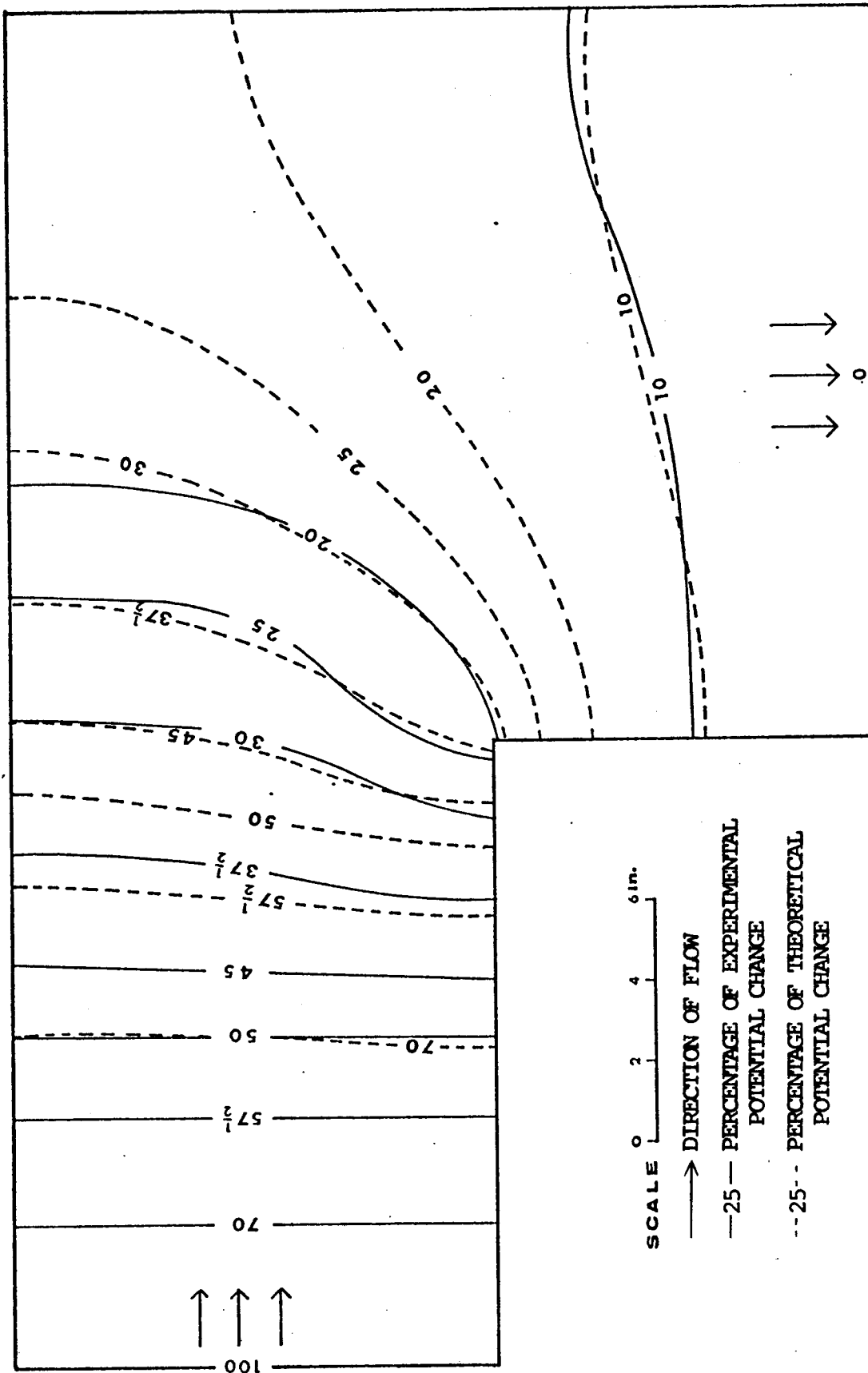


FIG. 12.- DISTRIBUTION OF THEORETICAL AND EXPERIMENTAL EQUIPOTENTIAL LINES FOR FLOW PAST A SHARP CORNER

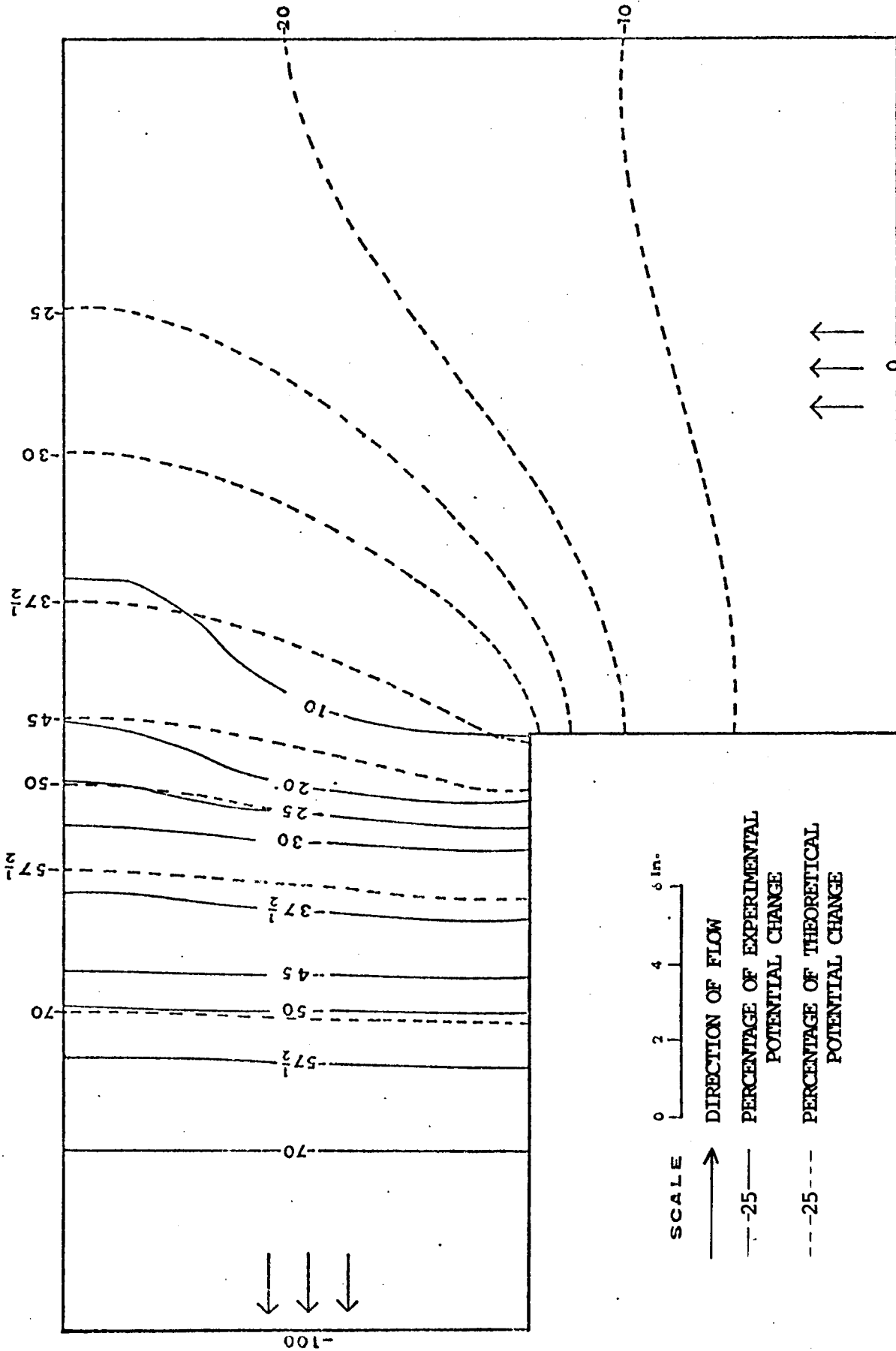


FIG. 13.- DISTRIBUTION OF THEORETICAL AND EXPERIMENTAL EQUIPOTENTIAL LINES FOR FLOW PAST A SHARP CORNER

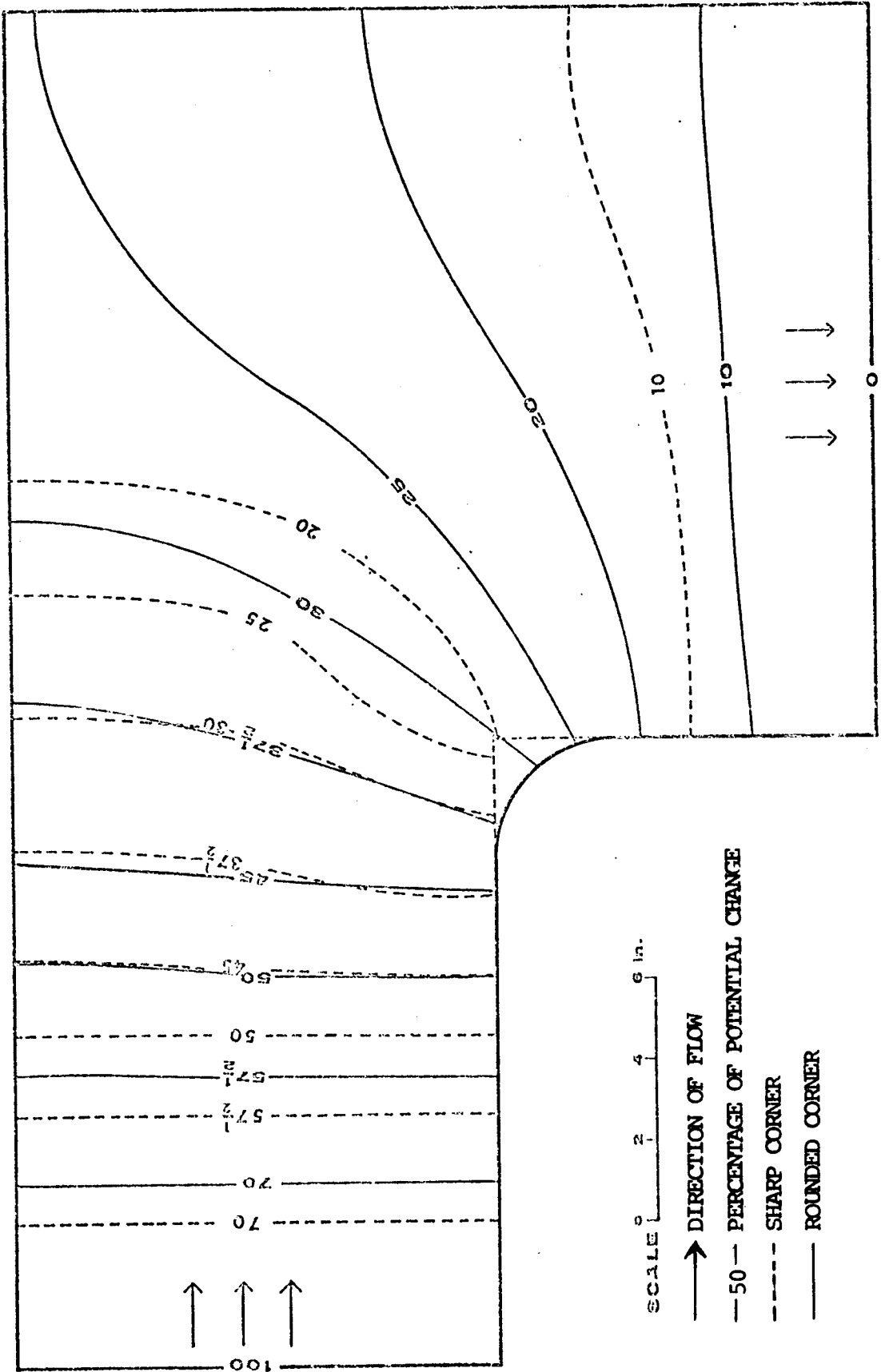


FIG. 14.- DISTRIBUTION OF EXPERIMENTAL EQUIPOTENTIAL LINES FOR FLOW PAST SHARP AND ROUNDED CORNERS

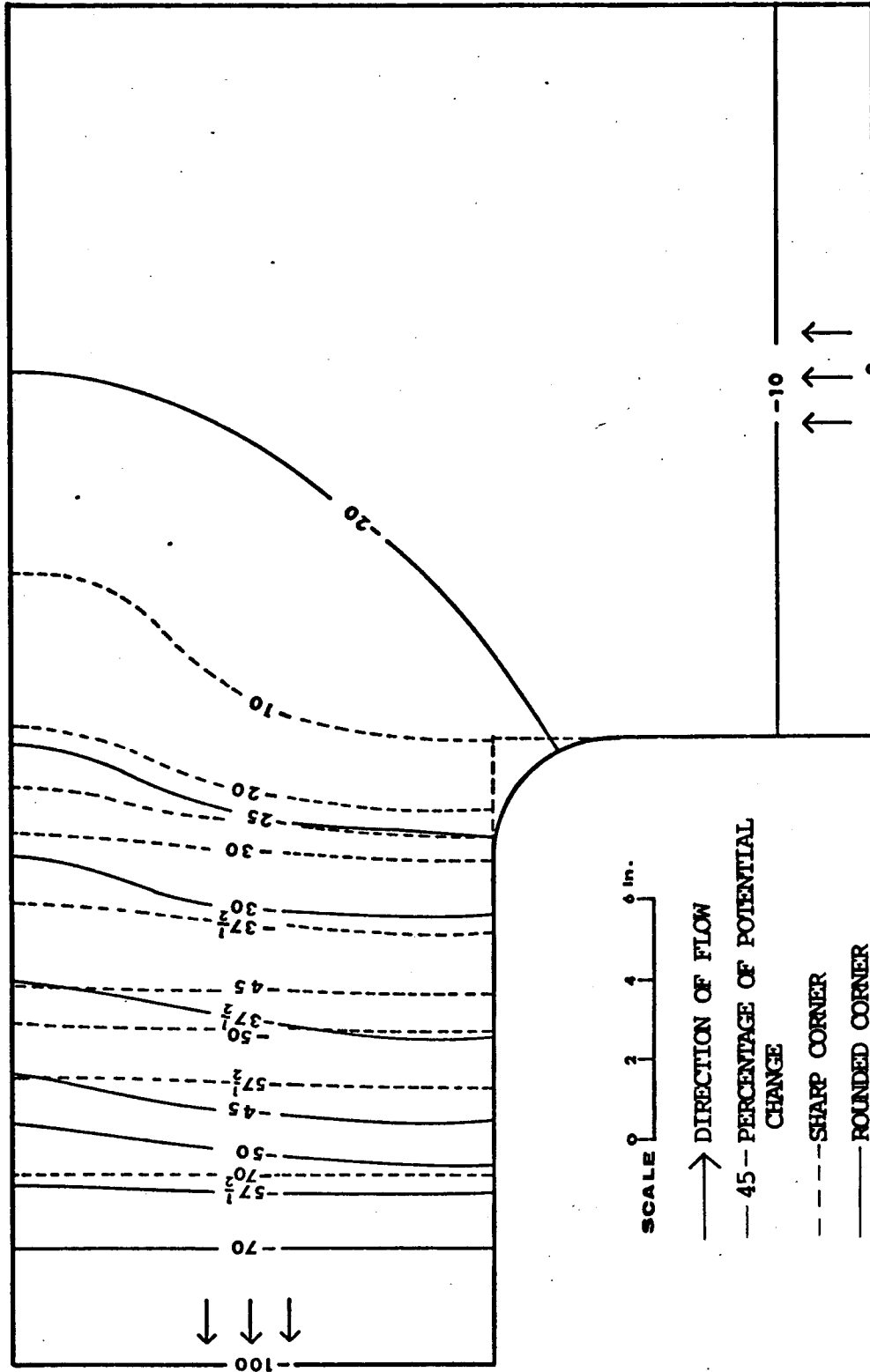


FIG. 15. - DISTRIBUTION OF EXPERIMENTAL EQUIPOTENTIAL LINES FOR FLOW PAST SHARP AND ROUNDED CORNERS

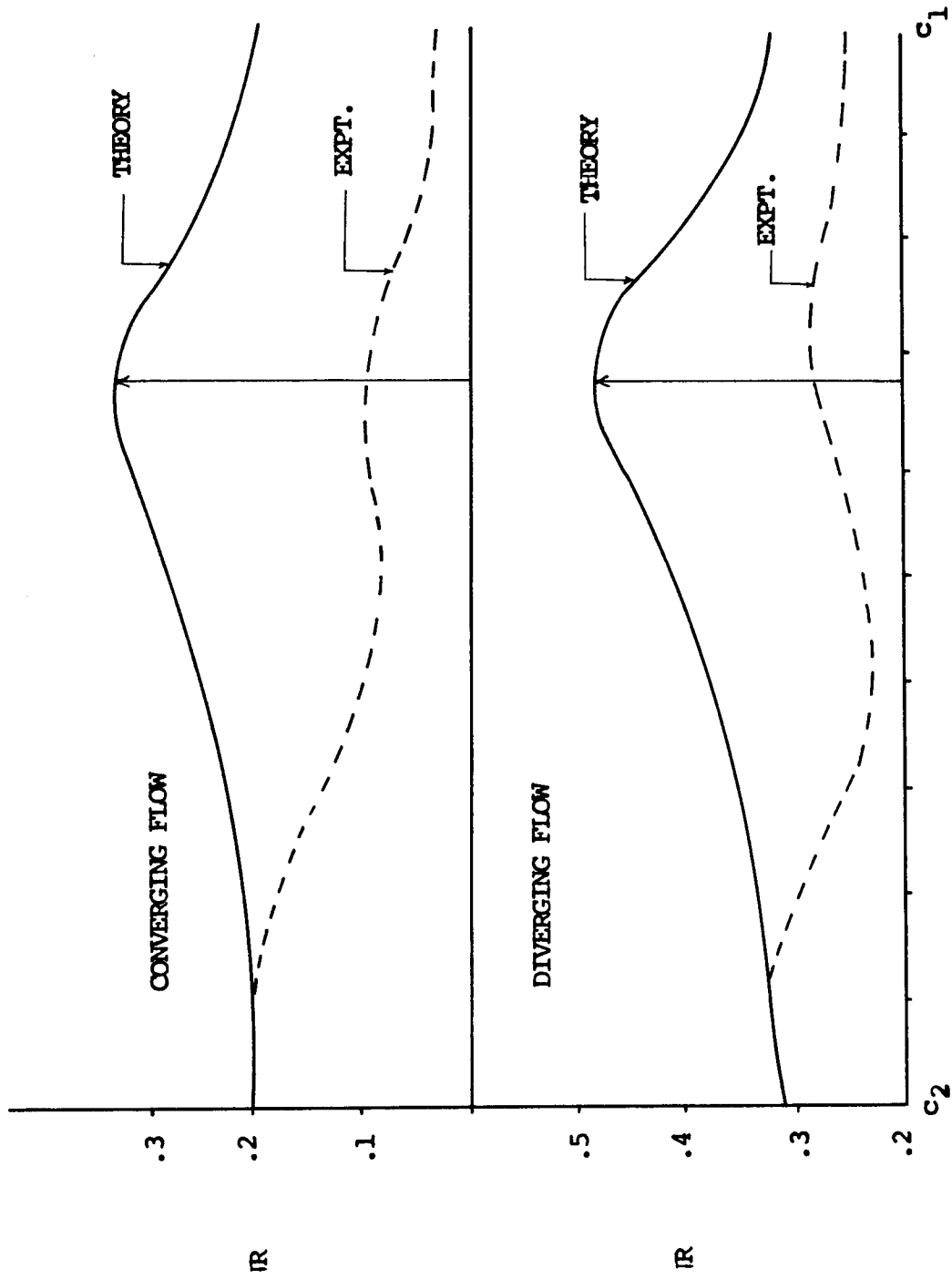


FIG. 16. - VARIATION OF EXPERIMENTAL AND THEORETICAL REYNOLDS NUMBERS ALONG THE SIDES OF THE MODEL WITH A ROUNDED CORNER

CHAPTER VI

DISCUSSION AND CONCLUSIONS

The distribution of experimental equipotential lines for the diverging flow past the rounded corner seem to agree fairly well with the theoretical equipotential lines in Fig. 10. There is, however, relatively poor agreement between the theoretical and experimental equipotential lines for the converging flow in Fig. 11.

There is poorer agreement between the patterns of theoretical and experimental equipotential lines for converging or diverging flows past the sharp corner in Figs. 12 and 13. Again, however, this agreement is relatively better for the diverging flow than for the converging one. Thus, there is better agreement between the theory and experiment for flow past a rounded corner than for the flow past a sharp corner, and the best agreement in either case is obtained when the streamlines diverge.

The diverging flows appear to distribute the potential drops more uniformly throughout the flow region, as shown in Fig. 14. However, the converging flows tend to concentrate the potential drops in the narrowest region of high velocities, as shown in Fig. 15.

The agreement between theoretical and experimental variation of the Reynolds number, as shown in Fig. 16, is poor for either converging or diverging flows. It should be noted, however, that neither the experimental nor the theoretical Reynolds number exceeded unity anywhere in the flow past the rounded corner. Hence, according to previous investigators, Darcy's law should have been valid and agreement between theory and experiment should have been better. This leads the writer to conclude that

either (1) Darcy's law does not accurately describe seepage in regions where streamlines diverge or converge rapidly or (2) some experimental error was responsible for part of this discrepancy between theory and experiment. The writer believes that the most likely source of experimental error was the possible separation of the Plexiglas top from the aquifer. Although precautions were taken during the construction stage, the possibility of separation during the experiment cannot be ruled out.

The interesting result that Darcy's law appears more nearly valid when streamlines are diverging rather than converging is exactly opposite to what has been found by many investigators in the potential flow theory of classical fluid mechanics. If no porous medium was present in these experiments, the Laplace equation would describe the converging flow much more accurately than the diverging flow. This is largely because flow separation is much more likely to occur when streamlines diverge. However, it is difficult, if not impossible, to interpret the results of experiments in flow through porous media in terms of classical irrotational flow theory. This is chiefly because acceleration terms in the equations of motion are so small compared to viscous resistance terms that they can be neglected for most flow through porous media. On the other hand, acceleration terms in classical irrotational fluid mechanics are so large compared to viscous resistance terms that the latter terms are neglected. The writer does not believe that flow separation could have occurred in these experiments because, by Darcy's law, this would have caused almost zero piezometric head gradients in a region of separation downstream of the sharp corner, and such a region was not observed.

BIBLIOGRAPHY

1. Aravin, V. I. and Numerov, S. N., Theory of Fluid Flow in Undeformable Porous Media, (Translated from Russian by Israel Program for Scientific Translations), Jerusalem, 1965.
2. Babbitt, H. and Caldwell, D. H., The Free Press Surface Around and Interference Between Gravity Wells, University of Illinois Eng. Exp. Sta. Bull. 374, 1948.
3. Darcy, H., Les fontains publiques de la Ville de Dijon, Paris, 1856.
4. Dupuit, J., "Etudes theoriques et pratiques sur le mouvement des eaux dans les canaux decouverts et a travers les terrains permeables," Paris, 1863.
5. Forchheimer, P. H., "Wasserbewegung durch Boden," Z. Ver. dt. Ing. 1901, p. 1782.
6. Harr, M. E., Groundwater and Seepage, San Francisco, McGraw-Hill 1962.
7. Harza, L. F., Uplift and Seepage under Dams on Sand, Trans. Am. Soc. Civil Engrs., Vol. 100, 1935.
8. Hunt, B. W., Discussion of Reference (20), ASCE Journal of the Hydraulics Division, January, 1969, p. 570.
9. Lindquist, E., "On the Flow of Water through Porous Soil," Report to the First Congress on Large Dams, Vol. 5, Stockholm, 1933, pp. 81-101.
10. Missbach, A., Listy Cukrova, Vol. 55, 1937, p. 293
11. Morcom, A. R., "Fluid Flow Through Granular Materials," Transactions, Institute of Chem. Engrs., Vol. 24, 1946, pp. 30-43.
12. Muskat, M., The Flow of Homogeneous Fluids through Porous Media, New York, McGraw-Hill, 1937.
13. Parkin, A. K., "Rockfill Dams with Inbuilt Spillways, Part I -- Hydraulic Characteristics," Bulletin No. 6, Water Research Foundation of Australia, 1963.
14. Polubarinova-Kochina, P. Ya., Theory of Groundwater Movement, Translated from Russian by J. M. Roger de Wiest, Princeton University Press, Princeton, 1962.

15. Rel'tov, B. F., Study of Seepage in Spatial Problems by Electrical Analogues, Izv. NIIG, 1935. Also Trans. 2nd Congr. on Large Dams, Wash, Vol. 5, 1936.
16. Slichter, C. S., "Theoretical Investigation of the Motion of Groundwaters," 19th Annual Report, U.S. Geol. Survey, Part 2, 1897-1898, pp. 329.
17. Todd, D. K., Investigation of Unsteady Flow in Porous Media by Means of a Hele-Shaw Viscous Fluid Model," thesis presented to the University of California, Berkeley, in 1953, in partial fulfillment of the requirements for the degree of Doctor of Philosophy.
18. Volker, R. E., "Nonlinear Flow in Porous Media by Finite Elements," ASCE Journal of the Hydraulics Division, November, 1969, pp. 2093.
19. Ward, J. C., "Turbulent Flow in Porous Media," Journal of the Hydraulics Division, ASCE, Vol. 90, No. HY5, Proc. Paper 4019, Sept., 1964, pp. 1-13.
20. Wright, D. E., "Nonlinear Flow through Granular Media," ASCE Journal of the Hydraulics Division, July 1968, pp. 851.
21. Wyckoff, R. D. and Reed, D. W., Electrical Conduction Models for the Solution of Water Seepage Problems, J. Appl. Phys., Vol. 6, 1935.
22. Zhukovskii, N. E., "A Theoretical Investigation on the Movement of Subsurface Water," (1889), Collected Works, Vol. III, Gostekhizdat (State Press), 1949.